Comparison of achievable performances as regards rubidium gas cell frequency standards with continuous and pulse laser pumping and with coherent population trapping

V. Zholnerov[1], A. Besedina[1], G.Kazakov[2]

[1]*The Russian Institute of Radionavigation and Time PJSC, 2 Rastrelli sq., St.-Petersburg 191124, RUSSIA, E-mail: office @ rirt.ru*
[2]*St. Petersburg's Technical University, 29 Politechnicheskaya street. St. Petersburg, 195251, RUSSIA*

We report the results of mathematical modeling the frequency stability for three types of rubidium gas cell frequency standards : with continuous and pulse laser pumping and with coherent population trapping (CPT). A critical point for using laser pumping in RFS which defines essentially the frequency stability is the influence of laser emission's frequency fluctuations. The effect of these fluctuations on frequency stability of RFS variants' considered is analyzed. Based on studies performed, the achievable stability for these RFS variants are compared.

I. INTRODUCTION

Using laser pumping enables one to improve in principle a frequency stability of the rubidium frequency standard (RFS) based on a gas cell. Many works of various authors give the results of RFS studies on three directions:

- with using a double radio-optical resonance signal in continuous laser pumping;
- with using a resonance signal Ramsey's structure in pulse laser pumping;
- with using a coherent population trapping (CPT) effect.

The main sources of RFS instability are considered in many works [1-7]. These works show that the matter-of-principle limiting factors are light shift and laser's frequency noise.
The clock's instability related to the light shift can be reduced by optimizing absorption cell (size, buffer mix, buffer gas pressure and temperature), pumping light's intensity and fluctuation level, by improving a laser frequency control technique (frequency, modulation index) as well as by using methods for suppression of the light shift [8]. The problem of laser's frequency noise impact of the RFS instability was studied, for the most part, at the theoretical level [3,4,10,11]. The role of optical pumping was shown as regards the FM-AM noise conversion on the contour of optical absorption line of atomic vapour with buffer gases.
Along with it, at present there is no the comparative analysis of achievable performances as regards RFS's of types mentioned above. Such an analysis is made in this paper.

1I. MULTI-PARAMETRIC OPTIMIZATION OF RFS WITH CONTINUOUS LASER PUMPING

The objective for RFS multi-parametric optimization is a calculated estimate of optimal standard's parameters providing the best frequency stability.

Numerical calculations show that a figure of merit dependence on temperature and length of gas cell T_c, L_c, pressure of buffer mix P_c, power and frequency detuning of laser emission J_{input}, ΔF_L , Rabi frequency R_{12} and frequency deviation of low frequency square wave modulation of microwave field Δ quantities is of extremal nature.
We can use a mean Allan variance as a criterion for complex optimization of RFS over the predefined measurement time interval:

$$\Xi = \frac{1}{\tau_2 - \tau_1}\int_{\tau_1}^{\tau_2}\sigma(\tau, F, D_1, D_2, \ldots, \Omega_0)d\tau \quad (1)$$

In the same time the interval $[\tau_1, \tau_2]$ is usually quite broad, so, to level off weights of short-term and long term frequency stability, it is advisable to use log-log scale and define a generalized figure of merit of RFS as a criterion for complex optimization given by the following expression :

$$Z(\tau_1, \tau_2) = \frac{1}{\log(\tau_1 / \tau_2)}\int_{\log\tau_1}^{\log\tau_2}\log[\sigma(\tau)]d(\log\tau) \quad (2)$$

This criterion is a surface under the $-\log[\sigma(\tau)]$ curve in function of $\log\tau$ over $[\tau_1, \tau_2]$ specified time interval.

In order to perform calculations, the computer program OPTIM.CPP was developed written in C++ System. The program core is a kinetic equations system in the Vanier-Audoin's form for optical pumping. This system was complemented with the equation for optical emission transfer [9].

For numerical solving these integro-differential equations gas cell was being divided into 'n' layers of sufficiently small elongation along the light propagation direction. Within such a layer pumping rates, light shift and absorption coefficient can be considered constant quantities. For each layer such values were computed as local values of pumping rates, light shift and absorption coefficient. The population values required for calculation of absorption coefficient are solutions of kinetic equation system.
This program OPTIM.CPP comprises a subprogram for global optimization which performs search of a set of optimal values of RFS parameters providing a maximum value of the RFS generalized figure of merit through a technique of coordinate-by-coordinate lift. This technique involves a cyclic procedure for searching optimal value of each parameter using the "golden cut" method with remaining parameter values obtaining during the previous step. Within each cycle optimal values of the microwave excitation parameter and deviation of microwave field frequency are found and values of differential parametric frequency shifts of the clock atomic transition are also calculated.

The following dimensions of the gas cell were selected: length of 20 mm, diameter of 20 mm. The N_2 + Kr mix was selected as a buffer mix. The parameters of spectral densities as regards fluctuations of gas cell temperature, constant magnetic field, phase fluctuations of microwave field, power of the microwave field and parameters of crystal oscillator's inherent instability were selected based on capabilities of the existing electronics.

The measurement of spectral density of laser emission power fluctuations for value of injection current 58.9 mA show the flicker behaviour of these fluctuations. The regression analysis of experimental data by analytical expression

$$S_{\Delta J/J}(\Omega) = \frac{A}{\Omega^2} + \frac{B}{\Omega} + C$$

gives the following values of constants : A=$7.38\cdot10^{-7}$, B = $1.63\cdot10^{-7}$, C = $1.8\cdot10^{-9}$ for I_l = 52.9 mA.
Our previous results of RFS optimization [10] didn't take into account the influence of FM-AM and FM-FM conversions on the performances of RFS. So it is interesting to compare these results with the results of optimization with taking into account these conversions. For this purpose more detailed multi-factor optimization of RFS was performed for the most promising scheme of continuous laser pumping shown in Fig. 1.
The kinetic equations of optical pumping for this scheme are as follows :

$$\frac{\partial\sigma_{11}}{\partial t} = \frac{1}{8}\rho - \gamma_1\sigma_{11} + \frac{\gamma_1}{8} \quad (3a)$$

$$\frac{\partial\sigma_{22}}{\partial t} = \frac{1}{8}\rho - \gamma_1\sigma_{22} + \frac{\gamma_1}{8} + 2R_{26}\psi \quad (3b)$$

$$\frac{\partial\sigma_{33}}{\partial t} = \frac{1}{8}\rho - \gamma_1\sigma_{33} + \frac{\gamma_1}{8} \quad (3c)$$

$$\frac{\partial\sigma_{44}}{\partial t} = -W_{44}\sigma_{44} + \frac{1}{8}\rho - \gamma_1\sigma_{44} + \frac{\gamma_1}{8} \quad (3d)$$

$$\frac{\partial\sigma_{55}}{\partial t} = -W_{55}\sigma_{55} + \frac{1}{8}\rho - \gamma_1\sigma_{55} + \frac{\gamma_1}{8} \quad (3e)$$

$$\frac{\partial\sigma_{66}}{\partial t} = -W_{66}\sigma_{66} + \frac{1}{8}\rho - \gamma_1\sigma_{66} + \frac{\gamma_1}{8} - 2R_{26}\psi \quad (3f)$$

$$\frac{\partial\sigma_{77}}{\partial t} = -W_{77}\sigma_{77} + \frac{1}{8}\rho - \gamma_1\sigma_{77} + \frac{\gamma_1}{8} \quad (3g)$$

$$\frac{\partial\sigma_{88}}{\partial t} = -W_{88}\sigma_{88} + \frac{1}{8}\rho - \gamma_1\sigma_{88} + \frac{\gamma_1}{8} \quad (3h)$$

$$\frac{\partial\varphi}{\partial t} = -\left(\gamma_2 + \frac{W_{66}}{2}\right)\varphi + \delta\psi \quad (3i)$$

$$\frac{\partial\psi}{\partial t} = -\left(\gamma_2 + \frac{W_{66}}{2}\right)\psi - \delta\varphi + R_{26}(\sigma_{66} - \sigma_{22}) \quad (3j),$$

where
$\rho = W_{44}\sigma_{44} + W_{55}\sigma_{55} + W_{66}\sigma_{66} + W_{77}\sigma_{77} + W_{88}\sigma_{88}$:
$W_{44} = W_1 + W_2 + \Gamma_1 + \Gamma_7$;
$W_{55} = W_3 + W_4 + \Gamma_2 + \Gamma_8 + \Gamma_9$;
$W_{66} = W_5 + W_6 + \Gamma_3 + \Gamma_4 + \Gamma_{10} + \Gamma_{11}$;
$W_{77} = W_7 + W_8 + \Gamma_5 + \Gamma_{12} + \Gamma_{13}$;
$W_{88} = W_9 + W_{10} + \Gamma_6 + \Gamma_{14}$ - rates of pumping 4-8 Zeeman's sublevels; φ and ψ - real and imaginary parts of the microwave coherence
$\sigma_{26} = (\varphi + i\psi)e^{i\omega t}$, R_{26} - Rabi frequency for $|\Phi_1,0\rangle \leftrightarrow |\Phi_2,0\rangle$ transition under action of the microwave field magnetic component
$\vec{H}_{\sim} = \vec{e}_\lambda \lambda \cos[\omega t + \xi(t)]; \xi(t)$ - phase modulation of the microwave field; $\delta = \omega - \omega_{62}$ - detuning of the microwave field frequency relative to the frequency of the clock transition, $|\Phi_1,0\rangle \leftrightarrow |\Phi_2,0\rangle$, γ_1 and γ_2 -

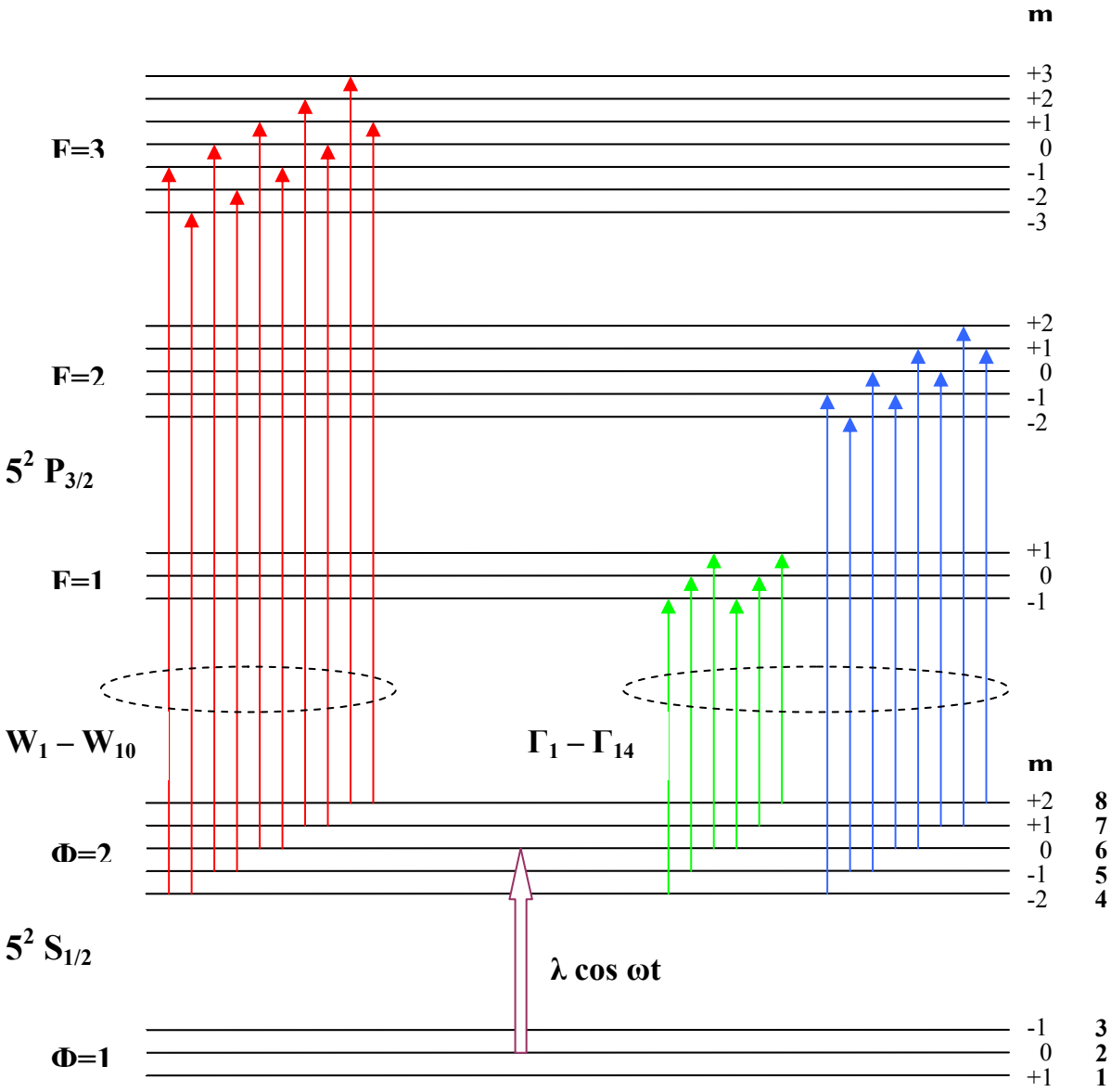

Fig. 1. . Laser pumping scheme used for analysis of continuous laser pumping

Table 1

Variant	P_{N_2} / P_{Kr}	P_c, Torr	T_c, K	ΔF_L, MHz	P_L, W/m^2	ΔF_{mod}, Hz	Z
Variant 1	1.214	4.24	319.2	139.91	0.11	160.6	13.202
Variant 2	1.241	15.0	325.0	213.17	0.04	102.6	13.198
Variant 3	1.263	15.0	333.0	213.43	0.055	213.4	13.177
Variant 4	1.241	20.0	325.0	250/28	0.025	250.3	13.148

rates of longitudinal and transverse relaxation in the ground state which magnitudes are adopted equal :

$$\gamma = \frac{4P_A\sigma_A}{\sqrt{\pi kTm_A}} + \left[\left(\frac{\pi}{L}\right)^2 + \left(\frac{2.405}{r}\right)^2\right]\frac{P_0/P_M}{\sum_{i=1}^{k}\frac{x_i^2}{D_{0i}}\sqrt{\frac{T_{0i}}{T}}} + \sum_{i=1}^{k}\sqrt{\frac{8(m_i+m_A)}{\pi kTm_im_A}}P_M x_i\sigma_i$$

The results of optimization are presented in Table 1. The variant 1 corresponds to searching an optimum for all parameters. The obtained values for buffer mixture's pressure and gas cell's temperature are too small. The model developed for the atomic discriminator is on the verge of confidence with such parameters' values. In addition, such a value of cell's temperature is not acceptable from the standpoint of operating conditions. Therefore, as regards variants 2, 3 and 4, cell's temperature and buffer mixture's pressure were excluded from a number of parameters being optimized and preset to the reasonable values.

Fig. 2 demonstrates frequency stability for all four variants without taking into account the fluctuations' conversions. Values of frequency stability for Variants 1 and 2 practically coincide whereas Variants 3 and 4 demonstrate the degradation of stability. Therefore one should select RFS parameters' values according to Variant 2.

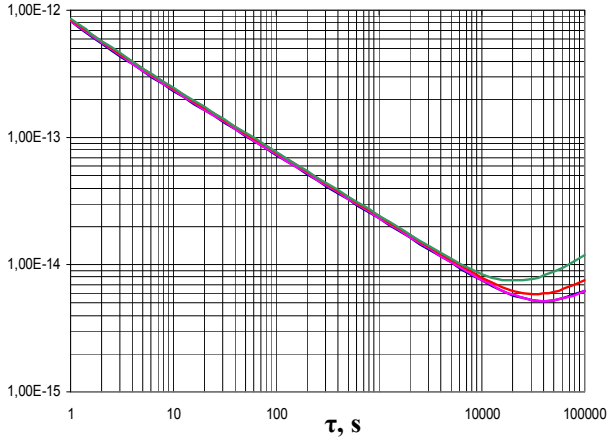

Fig 2. Frequency stability for RFS with continuous laser pumping in absence of FM-AM and FM-FM conversions. Variants 1,2 , Variant 3, Variant 4.

When using laser pumping in RFS, the key point is the presence of laser emission's frequency fluctuations. The effect of these fluctuations on RFS frequency stability shows itself in two directions. On the one hand, these fluctuations are being converted into fluctuations of the atomic discriminator's output signal on the optical absorption line (FM-AM). The other channel is the conversion of laser emission's frequency fluctuations into fluctuations of clock transition's frequency through a light shift (FM-FM).

Fig. 3 shows curves for RFS frequency stability after the multi-factor optimization with taking into account laser emission's frequency fluctuations for the Variant 2. In so doing, Curve 1 corresponds to the consideration for FM-AM conversion only. In this case, the stability degradation is not observed, for the laser can be tuned to the frequency with a minimum conversion of this type.

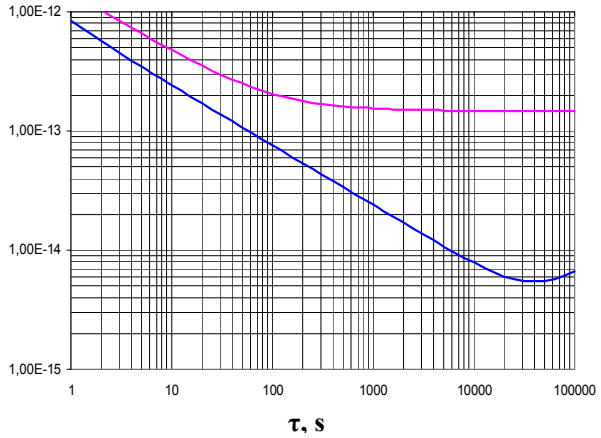

Fig. 3. Frequency stability for RFS with continuous laser pumping taking into account the effect of laser emission's frequency fluctuations. - Curve 1, - Curve 2

Curve 2 corresponds to the consideration for both conversion channels. One observes a significant degradation of frequency stability. The reason for such a degradation is the fact that laser's frequency corresponding to the minimum FM-AM conversion does not coincide with a laser frequency supporting the minimum light shift of the clock transition's frequency/

Of all known techniques for lowering a light shift value the use of pulse pumping is the most efficient one. So, we need to study this technique more detailed.

III. PULSE LASER PUMPING IN RFS

The action of optical pumping light on rubidium atoms causes, along with useful effect on creation of the population difference for the ground state sublevels, a shift of the atomic clock transition's frequency. The most efficient way for significant lowering of light shift in RFS is using of pulse pumping [11,12]. In this technique, action of pumping light and RF field is separated in. Over time intervals of t_p – duration the atoms are subjected to the pumping light action. After

this the pumping light is switched off, and the first RF field's pulse of t_R –duration is switched on. Then the RF field is switched off, and the atoms evolve freely over a t_f – time interval, after which the second RF field's pulse is switched on again. With this pulse completed, the pumping light is again switched on for the t_d – time interval to detect a signal of Ramsey-type. As far as pulses of pumping and detection follow each other, then, consequently, over a time interval of $t_d + t_p$, the RF coherence of the atomic ensemble responsible for appearance of the light shift is totally being destroyed.

The attempts to realize a principle of pulse optical pumping in the traditional RFS with spectral lamp were confronted by significant difficulties related to the impossible efficient realization of pulse operating mode for spectral lamp. Recently, due to the appearance of lasers of the needed wavelength for realization Rb^{87} vapor optical pumping, a new opportunity came to existence to use pulse optical pumping in RFS [13-15].

In works [13-15], the signal detection is realized by observing a microwave cavity's dispersion characteristic. In so doing, in order to obtain a needed signal value, one should provide a high value for loaded cavity's Q-factor. In this case, the special kinds of glass are needed for manufacturing a gas cell's bulb (for example, quartz glass), and this complicates significantly a technology for gas cell manufacturing. On the other hand, a large increase in cavity's Q-factor results in increase of frequency shifts connected with pilling of the atomic clock transition's frequency by the cavity's frequency. This causes the degradation of RFS accuracy parameters. Therefore, in spite of some loss in resonance signal value, it is advisable to realize a signal detection using the absorption of optical pumping light in the gas cell.

For finding optimal regimes for RFS with pulse laser pumping, theoretical studies and computer simulation of such RFS parameters are performed.

In the case when pumping is being performed from the upper level of the ground state, |F=2>, the basic system of kinetic equations is written as follows:

$$\frac{\partial \rho_{н}}{\partial t} = -\gamma\rho_l + \frac{P\Gamma}{8}(4\rho_u + \rho_{66}) + \frac{\gamma}{8}$$

$$\frac{\partial \rho_u}{\partial t} = -(P\Gamma + \gamma)\rho_u + \frac{P\Gamma}{8}(4\rho_u + \rho_{66}) + \frac{\gamma}{8}$$

$$\frac{\partial \rho_{22}}{\partial t} = -\gamma\rho_{22} + \frac{P\Gamma}{8}(4\rho_u + \rho_{66}) + \frac{\gamma}{8} + 2E\Lambda\psi$$

$$\frac{\partial \rho_{66}}{\partial t} = -(P\Gamma + \gamma)\rho_{66} + \frac{P\Gamma}{8}(4\rho_u + \rho_{66}) + \frac{\gamma}{8} - 2E\Lambda\psi$$

$$\frac{\partial \varphi}{\partial t} = -\left(P\frac{\Gamma}{2} + \gamma\right)\varphi + \delta\psi$$

$$\frac{\partial \psi}{\partial t} = -\left(P\frac{\Gamma}{2} + \gamma\right)\psi - \delta\varphi + E\Lambda(\rho_{66} - \rho_{22}),$$

where $P = \begin{cases} 1 \to t \in [0, t_d + t_p] \\ 0 \to t \in [t_d + t_p, t_d + t_p + 2t_R + t_f] \end{cases}$,

$$E = \begin{cases} 0 \to t \in [0, t_d + t_p] \\ 1 \to t \in [t_d + t_p, t_d + t_p + t_R] \cup \\ [t_d + t_p + t_R + t_f, t_d + t_p + t_R + t_f + t_R] \end{cases}$$

$\rho_l = \rho_{11} = \rho_{33}$, $\rho_u = \rho_{44} = \rho_{55} = \rho_{77} = \rho_{88}$ - populations of Zeeman's sublevels of ground state's upper and lower levels not interacting with RF field; $\rho_{26} = \varphi + i\psi$ - hyperfine coherence; Γ - pumping rate; γ - rate of longitudinal and transverse relaxation caused by Rb^{87} atom's interaction with a buffer gas and rubidium atom's diffusion to the cell walls within a buffer medium; $\delta = \omega - \omega_{62}$ - detuning of RF field frequency relative to the frequency of the atomic clock transition; Λ - Rabi's frequency proportional to the RF signal power. The numeration of ground state's Zeeman's levels is being out in order of increasing energy.

The kinetic equations have explicit solutions for all time interval.

With respect to the multi-factor optimization of RFS with pulse laser pumping, OPION.CPP computer program is developed which is similar to OPTIM.CPP program described above with using a mathematical model of the atomic discriminator according to the kinetic equations for the same parameters of gas cell and RFS units as in OPTIM.CPP program.

Fig. 4 presents curves of frequency stability for RFS with laser pulse pumping according to the results of multi-factor optimization of its parameters

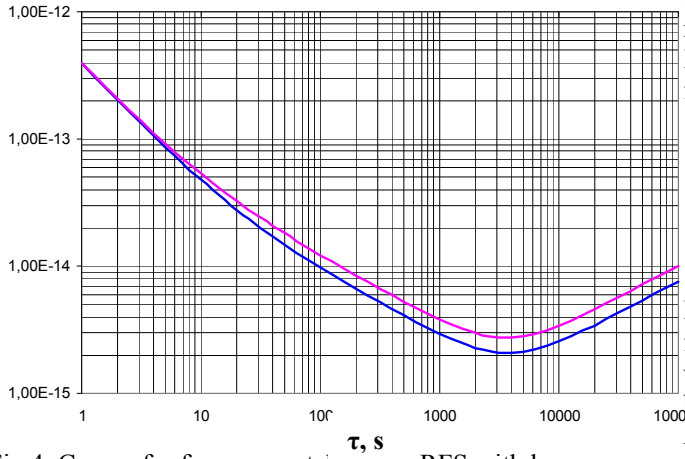

Fig 4. Curves for frequency stability of RFS with laser pulse pumping.

- without consideration for conversions of laser emission's fluctuations,

- with consideration for conversions of those fluctuations.

These curves show that the conversion of laser emission's frequency fluctuations affected the frequency stability negligibly small due to practically total zeroing a light shift of the atomic clock's frequency.

Some degradation of frequency stability within a long-term domain is due to low frequency fluctuations of atomic discriminator's parameters. Among the most pronounced sources of low-frequency fluctuations are following ones;

- fluctuations of gas cell's temperature;
- fluctuations of constant magnetic field;
- fluctuations of RF field power.

This points to the need for special emphasis as regards supporting appropriate parameters for stabilizer of magnetic field solenoid's current and gas cell's thermoregulator as well as technology for manufacturing of gas cells.

III. RFS WITH CPT

When using CPT in rubidium gas cell frequency standard, there is no need in using a microwave cavity. This permits to reduce atomic discriminator's dimensions and to avoid technological complications connected with using and manufacturing such a cavity.

For theoretical evaluating the achievable values of standard's frequency stability in case of using the CPT effect, one should act as follows: to refine the AFS block diagram as an automatic frequency lock system; to choose the optimal CPT scheme and to modernize a computer program for multiparametric RFS optimization created previously for DROR case with continuous laser pumping.

In the case of CPT, Rb^{87} atoms are affected by dual-frequency laser field

$$\vec{E}(\vec{r},t)=\vec{E}_0^1\exp\left[i\left(\nu_1 t-\vec{k}_1\vec{r}\right)\right]+\vec{E}_0^2\exp\left[i\left(\nu_2 t-\vec{k}_2\vec{r}\right)\right]+c.c.$$

There are three possible schemes for CPT realization:

- with circular polarization of laser fields;
- «lin || lin» configuration;
- «lin ⊥ lin» configuration.

Preliminary estimations show that the «lin ⊥ lin» configuration is more preferable, as far as in this case, when leveling the intensities of laser fields, it is possible to diminish a value of the light shift significantly. Along with it, the practical realization of this configuration presents certain difficulties. One of the possible methods for obtaining «lin ⊥ lin» configuration is given in [16].

The scheme of atomic transitions for the considered case is given in Fig.5.

Dual-frequency laser field excites 24 optical coherences and 7 microwave coherences. Total number the kinetic equations is equal 78. Substituting the equations for optical coherences into another equation we can reduce this number to 23. Some of microwave coherences: ρ_{17}, ρ_{24} ρ_{28}, ρ_{35} have frequencies that differ from the frequency of clock transition significantly. So we can neglect its influence on the central CPT signal. In this case the number of kinetic equation reduces to 15. These equations are the core of computer program OPCPT.CPP.

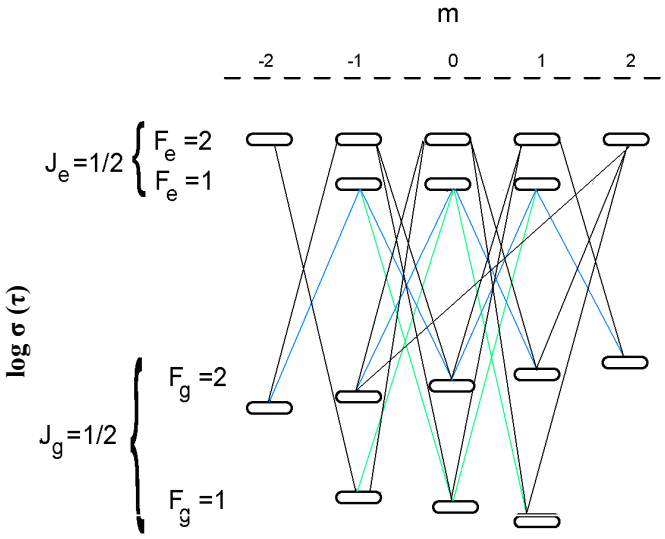

Fig. 5. Scheme of atomic transitions when affecting Rb^{87} atoms by the dual-frequency laser emission

Fig. 6 presents curves of frequency stability for RFS with CPT according to the results of multi-factor optimization of its parameters

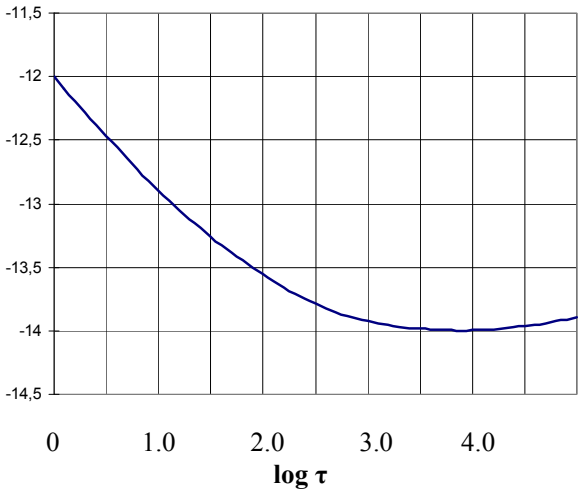

Fig.6. Frequency stability of RFS with CPT.

This curve shows that we could not achieve the long-term frequency stability better than $1 \cdot 10^{-14}$ for this type of this type of RFS. There are two explanations of this fact. Firstly, the value of light shift is not zeroing even for the case of «lin ⊥ lin» configuration. Secondly, the microwave coherences ρ_{15} and ρ_{37} affecting on the signal of CPT have the frequencies depending on the value of constant magnetic field in the first order. Thus the low frequency fluctuations of magnetic field reduce the long-term frequency stability of RFS with CPT.

IV. CONCLUSIONS

The FM-AM and FM-FM conversions in RFS with continuous laser pumping reduce the long-term frequency stability significantly.
The performances of RFS with pulse laser pumping are very promising. In this case one can achieve the long-term stability at the level $(2\text{-}3) \cdot 10^{-15}$.
In the case of RFS with CPT the long term frequency stability is not better than $1 \cdot 10^{-14}$.

Acknowledgements

We would like to acknowledge Dr. G. Mileti (LTF), Dr. J. Delporte (CNES) and Prof. B.G.Matisov (SPTU) for supporting this work and helpful discussions.

REFERENCES

[1] J.C. Camparo, R.P. Frueholz, "Fundamental stability limits for the diode-laser-pumped Rb atomic frequency standard", J. Appl. Phys., vol. 59, no. 10, pp. 3313-3317, 1986.

[2] G. Mileti, J. Deng, F.L. Walls, D.A. Jenning, and R.E. Drullinger, "Laser-Pumped Rubidium Frequency Standards: New Analysis and Progress", IEEE J. of Quantum Electronics, vol. 34, no.2, pp. 233-237, 1998.

[3] J.C. Camparo and W.F. Buell, "Laser PM and AM conversion in atomic vapors and short term clock stability", FCS, 1997, pp. 253-258, Orlando, FL, USA.

[4] J. Kitching, H.G. Robinson, and L. Hollberg, "Optical-pumping noise in laser-pumped, all-optical microwave frequency references", J. Opt. Soc. Am. B, vol. 18, no. 11, pp.1676-1683, 2001.

[5] C. Affolderbach, F. Droz, and G. Mileti, 35th Ann. PTTI Meeting, pp. 489-497, 2003 and reference therein.

[6] C. Affolderbach, F. Droz, and G. Mileti, "Experimental demonstration of a compact and high-performance laser-pumped Rb gas cell atomic frequency standard", IEEE Trans. Instrum. & Meas., vol. 55, no. 2, pp. 429-435, 2006.

[7] A.N. Besedina, O.V.Berezovskaya, A.G. Gevorkyan, G. Mileti, and V.S. Zholnerov, "Short and medium term frequency stability of a laser pumped rubidium gas-cell frequency standard for satellite navigation", Proc. of 20th EFTF, 2006, Braunschweig, Germany.

[8] C. Affolderbach, C. Andreeva, S. Cartaleva, T. Karaulanov, G. Mileti, and D. Slavov, "Light shift suppression in laser optically-pumped vapour-cell atomic frequency standards", Appl. Phys. B, Photophys. Laser Chem., vol. 80, no. 7, pp. 841-848, 2005.

[9] V. Zholnerov, O.Kharchev, "Analysis of passive atomic frequency standards stability", Proc. of the Joint Meeting 16th European Frequency & Time Forum and 2002 IEEE International Frequency Control Symposium, March 2002, St. Petersburg, Russia.

[10] A. Besedina, A. Gevorkyan, G. Mileti, V. Zholnerov, and A. Bassevich, "Preliminary results of investigation of the high-stable Rubidium atomic beam frequency standard with laser pumping/detection for space application", Proc. of the 20th EFTF, Braunschweig, Germany, 2006.

[11] E.I.Alexeyev, E.N.Bazarov, A.E.Levshin, "To the theory of a frequency standard with pulse optical pumping", Radiotechnics and Electronics, 1974, no. 1, pp. 103-110 (In Russian)

[12] E.I.Alexeyev, E.N.Bazarov, G.I.Telegin, "Light shifts in an atomic frequency standard with pulse optical pumping and optical indication of Ramsey's structure of Rb^{87} atom 0-0 transition", Radiotechnics and Electronics, 1975, no. 4, pp. 778-785 (In Russian)

[13] A. Godone, S. Micalizio, and F. Levi, "Pulsed optically pumped frequency standard", Physical Review A 70, 2004, pp. 023409-1 – 023409-11.

[14] A. Godone, S. Micalizio, C. E. Calosso and F. Levi, "The pulsed rubidium clock", IEEE Trans. on Ultrasonics, Ferroelectrics, and Frequency Control, vol. 53, No. 3, March 2006.

[15]F. Levi, S. Micalizio, A. Godone, C. E. Calosso and Elio, "Realization of a pulsed optically pumped rubidium frequency standard" Proceedings of the 20th. European Frequency and Time Forum, 2006. pp. 229-232.

[16]Y.-Y. Jau, E. Miron, A.B. Post, et al, PhysRevLett **93**, 160802 , 2004

This work was supported by the INTAS-CNES Project no. 06-1000024-9321